

Magnetoluminescence and magnetorefectance of the A exciton of CdS and CdSe

H. Venghaus, S. Suga,* and K. Cho†

Max-Planck-Institut für Festkörperforschung, 7000 Stuttgart 80, Federal Republic of Germany

(Received 21 March 1977)

Magnetoluminescence and magnetorefectance have been measured on the A exciton of CdS and CdSe in magnetic fields up to 12 T. In the case of CdS, we get the following results: For $\vec{H} \parallel \vec{c}$ the luminescence line at 2.553 eV, attributed to the Γ_6 triplet state splits into two components giving a g factor $|g_{h\parallel} + g_{e\parallel}| = 3.02 \pm 0.10$. From the directly measured difference between σ^- and σ^+ polarized light the g factor of the Γ_5 singlet state is determined as $g_{h\parallel} - g_{e\parallel} = -0.56 \pm 0.05$, and thus we derive the electron and hole g values $g_{e\parallel} = +1.79 \pm 0.10$ and $g_{h\parallel} = +1.23 \pm 0.10$. In luminescence with $\vec{E} \perp \vec{c}$ polarization and $\vec{H} \parallel \vec{c}$ a narrow line emerges with increasing magnetic field at energies below the Γ_5 luminescence peak. The additional line is attributed to the low-energy component of the Γ_6 triplet state. The most prominent feature of the magnetorefectance spectra is the appearance of an additional reflectance structure below the main reflectance minimum for $\vec{E} \perp \vec{c}$ and $\vec{H} \perp \vec{c}$. This structure is attributed to the triplet state becoming observable due to magnetic-field-induced mixing between the Γ_5 and Γ_6 states of the A exciton. From the diamagnetic shift of the Γ_6 state for $\vec{H} \parallel \vec{c}$ we derive $\mu_x = 0.16$, while $\mu_z = 0.185$ is obtained from the diamagnetic shift for $\vec{H} \perp \vec{c}$. In the case of CdSe we derive from magnetoluminescence the g value of the A exciton $|g_{h\parallel} - g_{e\parallel}| = 1.76 \pm 0.20$. The magnetorefectance spectra exhibit a corresponding splitting. The diamagnetic shift of the exciton structure yields reduced exciton masses $\mu_x = 0.096 \pm 0.01$ and $\mu_z = 0.112 \pm 0.010$. Mixing between the Γ_6 triplet and dipole allowed states is much less pronounced for CdSe than for CdS.

I. INTRODUCTION

Exciton states in CdS and CdSe received considerable attention more than ten years ago and have attracted renewed interest recently, in particular with respect to the exciton-polariton¹⁻⁴ and the excitonic molecule.^{5,6} A great deal of information has already been derived from early magneto-absorption and magnetorefectance measurements on the $n \geq 2$ exciton states,⁷⁻⁹ but further information can be obtained from the investigation of the exciton ground state, which has become the subject of magneto-optical experiments with the availability of powerful superconducting magnets.

In the present paper we report on magnetoluminescence and magnetorefectance experiments in the region of the free A exciton in CdS and CdSe. (Part of the reflectance data were already reported in Ref. 10). After a brief account of the experimental conditions in Sec. II, we present in Sec. III the relevant part of the theory, which describes the interaction between different exciton states by various mechanisms in a general way.¹¹ The experimental results are given and discussed in Sec. IV A (CdS) and Sec. IV B (CdSe). The main results are:

(i) for $\vec{H} \parallel \vec{c}$ the exciton states split as described by a linear Zeeman Hamiltonian, and the g values derived are in quantitative agreement with the results obtained by other authors from the investigation of excited states ($n \geq 2$). The same holds for exciton effective masses derived from the diamag-

netic shift (Secs. IV A 6 and IV B).

(ii) In the $\vec{E} \perp \vec{c}$, $\vec{H} \parallel \vec{c}$ configuration, a split component of the $\Gamma_6(A)$ triplet state was observed for the first time in the luminescence spectrum of CdS for $\vec{E} \perp \vec{c}$ polarization. The model of the k -linear mixing of the $\Gamma_6(A)$ and the $\Gamma_5(B)$ excitons is consistent with this result (Secs. IV A 3 and IV A 4).

(iii) The dipole-forbidden triplet state of the A exciton is also observed in reflectance for $\vec{E} \perp \vec{c}$ under the influence of a magnetic field $\vec{H} \perp \vec{c}$ both in CdS and CdSe. This is attributed to magnetic-field-induced mixing between singlet and triplet states of the A exciton. The effect is more pronounced in CdS than in CdSe (Secs. IV A 5 and IV B).

II. EXPERIMENTAL

Luminescence and reflectance in Voigt configuration were measured on high-purity vapor-grown CdS^{12, 13} and CdSe single crystals, which had the form of platelets with the crystal c axis parallel to the surface. The crystals were mounted strain free in a helium flow exchange-gas cryostat and cooled down to $\sim 4^\circ\text{K}$. Reflectance of CdS in Faraday configuration for $\vec{H} \parallel \vec{c}$ was measured on natural surfaces of slightly lower quality but larger crystals, having planes perpendicular to the c axis of approximately 1×1 mm size. In luminescence measurements on these larger crystals the free exciton line could be seen clearly, although less pronounced than in the case of the thin platelets.

The luminescence was excited by a He-Cd laser at 325 nm for CdS and at 441.6 nm for CdSe with less than 5 mW excitation power. Reflectance was measured with a quartz-iodine lamp. The detecting system consisted of a Spex $\frac{3}{4}$ -m single-grating monochromator, a photomultiplier tube (EMI 9658B) cooled with dry nitrogen gas and a lock-in amplifier (PAR HR8). The resolution of the monochromator was typically set to 0.3–0.5 Å.

III. THEORETICAL

A. General considerations

Before presenting the experimental data and their interpretation we will briefly discuss those terms of the exciton Hamiltonian which are relevant to the present experiments. We will confine ourselves to a compilation of theoretical results in a convenient form and give no derivation or detailed theoretical treatment, since this has already been done elsewhere.¹¹ The notations and definitions, if not otherwise specified, are based on Ref. 11, which included the formulation of Ref. 10 as a special case.

CdS has space group C_{6v}^4 with the hexagonal axis generally referred to as the c axis. The z axis of the Cartesian coordinate system (x, y, z) is chosen along the c axis. Without loss of generality, we take the exciton wave vector \vec{k} in the x, z plane [$\vec{k} \parallel (\xi, 0, \xi)$; $\xi^2 + \zeta^2 = 1$]. At $k = 0$, the lowest conduction band has Γ_7 symmetry, while the uppermost valence bands have symmetry Γ_9 , Γ_7 , and Γ_7 . Excitons associated with these valence bands are labeled A , B , and C exciton, respectively, and each exciton state has 4 sublevels. The A exciton consists of a twofold degenerate dipole allowed

TABLE I. Basis functions. Dipole matrix elements $\langle \psi | \vec{M} | 0 \rangle$ are given for light polarized along the (ξ, η, ζ) direction in relative units. The quasicubic parameters γ and δ ($\gamma^2 + \delta^2 = 1$) are defined in Ref. 11.

A-exciton		B-exciton		
ψ	Dipole matrix element	ψ	Dipole matrix element	
Γ_5	$ x\rangle_A$	ξ	$ x\rangle_B$	$\gamma\xi$
	$ y\rangle_A$	η	$ y\rangle_B$	$\gamma\eta$
Γ_6	$ t'\rangle_A$	0	$ z\rangle_B$	$\sqrt{2}\delta\xi$
	$ t\rangle_A$	0	$ t\rangle_B$	0

state having Γ_5 symmetry, observable with $\vec{E} \perp \vec{c}$ polarization and a twofold degenerate spin triplet state having Γ_6 symmetry, which is dipole forbidden in the absence of perturbations. The B and C excitons each decompose into substates having symmetry Γ_1 (dipole allowed with $\vec{E} \parallel \vec{c}$ polarization), Γ_2 (spin triplet, dipole forbidden), and Γ_5 (twofold degenerate, dipole allowed for $\vec{E} \perp \vec{c}$ polarization). The A - and B -valence bands are split by 16 meV (crystal field) and the spin-orbit split-off C band is 57 meV below the B band.¹⁴ Interactions between A - and C -exciton states are therefore neglected in the present paper.

With respect to the mixing and splitting of the A - and B -exciton states, we consider three different types of mechanism, namely (i) the electron-hole exchange, (ii) the linear Zeeman, and (iii) the diamagnetic interactions. In terms of the basis func-

TABLE II. Exchange-interaction and diamagnetic part of exciton Hamiltonian. Nondiagonal elements are given separately in the upper right (exchange interaction) and lower left (diamagnetic part) corners for the sake of clarity. The complete matrix is obtained adding the nondiagonal elements of the Hermitian-conjugate matrix.^a

$ x\rangle_A$	$ y\rangle_A$	$ t'\rangle_A$	$ t\rangle_A$	$ x\rangle_B$	$ y\rangle_B$	$ z\rangle_B$	$ t\rangle_B$
$D_1 + j(\xi)$	0	0	0	$\gamma j(\xi)$	0	$9\sqrt{2}j_1\xi\xi\delta$	0
	$D_1 + j(0)$	0	0	0	$\gamma j(0)$	0	0
		D_1	0	0	0	0	0
			D_1	0	0	0	0
$-d \begin{pmatrix} W & Z \\ Z & -W \end{pmatrix}$	$c \begin{pmatrix} -X & Y \\ Y & X \end{pmatrix}$	$D_2 + \gamma^2 j(\xi)$	0	$9\sqrt{2}j_1\xi\xi\gamma\delta$	0	0	0
			$D_2 + \gamma^2 j(0)$	0	0	0	0
$c \begin{pmatrix} -X & -Y \\ -Y & X \end{pmatrix}$	$d \begin{pmatrix} W & -Z \\ -Z & -W \end{pmatrix}$			$D_2 + 2\delta^2 j(\xi)$	0	0	0
							D_2

^a $D_i = a_i H_z^2 + b_i (H_x^2 + H_y^2)$ ($i=1, 2$), $W = H_x^2 - H_y^2$, $X = H_x H_z$, $Y = H_y H_z$, $Z = 2H_x H_y$.

tions given in Table I, the matrix for (i) and (iii) is given in Table II, where

$$j(u) = 3[j_0 + j_1(3u^2 - 1)] \quad (u = \xi, \zeta) \quad (3.1)$$

and j_0 and j_1 are the short- and long-range exchange constants, respectively.¹¹

The coefficients a_1 , a_2 , b_1 , b_2 , c , and d determine the diamagnetic effects. In a simple approximation, some of these coefficients can be expressed in terms of the more fundamental material parameters as⁹

$$a_1 = \frac{1}{m_0} \left(\frac{ea_0}{2c} \right)^2 \epsilon_x \epsilon_z \frac{1}{\mu_x^3} \quad (3.2)$$

and

$$b_1 = a_1 \mu_x / \mu_z, \quad (3.3)$$

where a_0 is the exciton radius, (ϵ_x, ϵ_z) and (μ_x, μ_z) are the (transverse, longitudinal) dielectric constant and effective reduced mass, respectively. The latter is defined as

$$\frac{1}{\mu_i} = \frac{m_0}{m_{e_i}^*} + \frac{m_0}{m_{h_i}^*} \quad (i = x, z). \quad (3.4)$$

The matrix for the linear Zeeman interaction is given in Table III.

The correspondence to the results in Ref. 10 is obtained by putting

$$\begin{aligned} g_{\parallel} &= g_{e\parallel}, \quad g_{\perp} = g_{e\perp}, \quad g_1 = g_{h\parallel}(A), \quad g_2 = g_{h\parallel}(B), \\ g_3 &= g_{h\perp}(B), \quad j(0) = \frac{1}{2}\Delta, \quad 2\delta^2 j(0) = \Delta_{\parallel}, \\ \gamma^2 j(0) &= \Delta_{\perp}. \end{aligned} \quad (3.5)$$

Note that the definition of $|t'\rangle_A$ and $|t\rangle_A$ are different from that of $|t_1\rangle$ and $|t_2\rangle$ used in Ref. 10, i.e.,

$$\begin{aligned} i|t'\rangle_A &= (|t_2\rangle - |t_1\rangle) / \sqrt{2}, \\ i|t\rangle_A &= (|t_2\rangle + |t_1\rangle) / \sqrt{2}. \end{aligned} \quad (3.6)$$

TABLE III. Linear Zeeman effect. The contributions from the conduction and valence bands are written in the lower left and upper right corners, respectively. The complete matrix is obtained by adding the Hermitian-conjugate matrix. (For definition of symbols g_i see text, Sec. II.)

	$ x\rangle_A$	$ y\rangle_A$	$ t'\rangle_A$	$ t\rangle_A$	$ x\rangle_B$	$ y\rangle_B$	$ z\rangle_B$	$ t\rangle_B$
	n							
	0	$-ig_{\perp}H_z$			0	0	$ig_4 \begin{pmatrix} H_y & -H_x \\ -H_x & H_y \end{pmatrix}$	
	$-ig_{\parallel}H_z$	0			0	0		
	$ig_{\perp} \begin{pmatrix} -H_y & -H_x \\ -H_x & H_y \end{pmatrix}$		0	ig_1H_z	$ig_4 \begin{pmatrix} H_y & H_x \\ H_x & -H_y \end{pmatrix}$		0	0
			$-ig_{\parallel}H_z$	0			0	0
					0	$-ig_2H_z$	$ig_3 \begin{pmatrix} -H_y & -H_x \\ H_x & -H_y \end{pmatrix}$	
					$ig_{\parallel}H_z$	0		
					$ig_{\perp} \begin{pmatrix} H_y & -H_x \\ -H_x & -H_y \end{pmatrix}$		0	ig_2H_z
$\frac{1}{2}\mu_B$							$ig_{\parallel}H_z$	0

B. Energy eigenvalues

Calculation of the eigenvalues using only the diagonal block for the A exciton (i.e., neglecting interactions between A - and B - or C -exciton states) yields the following results:

1. $\vec{H} \parallel \vec{c}$

For Γ_5 and Γ_6 one obtains

$$\begin{aligned} E_{\pm}(\Gamma_5) &= D_1 + \frac{1}{2}[j(\xi) + j(0)] \\ &\quad \pm \frac{1}{2}\{[j(\xi) - j(0)]^2 + (g_{\parallel} - g_1)^2 \mu_B^2 H^2\}^{1/2}, \end{aligned} \quad (3.7)$$

$$E_{\pm}(\Gamma_6) = D_1 \pm \frac{1}{2}|g_{\parallel} + g_1| \mu_B H. \quad (3.8)$$

2. $\vec{H} \perp \vec{c}$ ($H_x = H_z = 0$)

For $\vec{H} \perp \vec{c}$ the energies of the A -exciton states are given by

$$\begin{aligned} E_{\pm}(|y\rangle_A, |t\rangle_A) &= D_1 + \frac{1}{2}j(0) \\ &\quad \pm \frac{1}{2}[j(0)^2 + (g_{\perp} \mu_B H)^2]^{1/2} \end{aligned} \quad (3.9)$$

$$\begin{aligned} E_{\pm}(|x\rangle_A, |t'\rangle_A) &= D_1 + \frac{1}{2}j(\xi) \\ &\quad \pm \frac{1}{2}[j(\xi)^2 + (g_{\perp} \mu_B H)^2]^{1/2} \end{aligned} \quad (3.10)$$

As can be seen from (3.7), (3.9), and (3.10) a linear Zeeman splitting of Γ_5 states occurs only for $\vec{H} \parallel \vec{c}$ and $\vec{k} \parallel \vec{c}$ ($\xi = 0$), or can be expected to a good approximation, if

$$j(\xi), j(0) \ll g_{\perp} \mu_B H \quad \text{or} \quad (g_{\parallel} - g_1) \mu_B H \quad (3.11)$$

holds.

C. Selection rules for $\Gamma_{5L}(A)$ and $\Gamma_6(A)$

The basis states $|t\rangle_A$, $|t'\rangle_A$ and $\Gamma_{5L}(A)$ [longitudinal state of $\Gamma_5(A)$] in the case of $\vec{k} \perp \vec{c}$ are opti-

cally forbidden. In certain configurations, however, they can be weakly observed without any external perturbation, and this is interpreted as being due to the finiteness of the exciton wave vector.⁸

The perturbation-induced mixing of different states can be derived for any perturbation from the matrices given in Tables II and III, if H is replaced by the perturbation under consideration. For a detailed general discussion see Ref. 11. The relevant part of the selection rules can be summarized as follows: $\Gamma_{5L}(A)$ can be observed for $\vec{E} \parallel \vec{z}$ (i.e., $\vec{E} \parallel \vec{c}$) due to nonzero k_x or H_y , for example. For $\vec{E} \parallel \vec{y}$ (i.e., $\vec{E} \perp \vec{c}$) the $\Gamma_{5L}(A)$ state becomes partly allowed in the presence of nonzero H_z , $H_x H_y$, or $k_x k_y$, for example.

The $\Gamma_6 A$ -exciton triplet states become allowed for $\vec{E} \parallel \vec{c}$ polarization by Γ_6 -type perturbations like $(k_x^2 - k_y^2, 2k_x k_y)$ and for $\vec{E} \perp \vec{c}$ polarization in the presence of nonzero (k_x, k_y) , (H_x, H_y) , or $(k_x k_x, k_y k_y)$, for example.

IV. RESULTS AND DISCUSSIONS

A. CdS

1. $\vec{H} \parallel \vec{c}$, $\vec{E} \parallel \vec{c}$, and $\vec{k} \perp \vec{c}$ luminescence

Luminescence spectra of CdS obtained for $\vec{E} \parallel \vec{c}$ polarization and $\vec{H} \parallel \vec{c}$ in the energy region of the A exciton are shown in Fig. 1. Two maxima observed at zero magnetic field have already been assigned to the Γ_6 spin triplet and the Γ_5 longitudinal state of the A exciton.⁸

Under the influence of a magnetic field parallel to the c axis the low-energy (Γ_6) line splits into two components, and according to (3.8) and (3.5) their energy separation is given by

$$\Delta E = |g_{h\parallel} + g_{e\parallel}| \mu_B H. \quad (4.1)$$

From the results shown in Fig. 1 we derive

$$|g_{h\parallel} + g_{e\parallel}| = 3.02 \pm 0.1. \quad (4.2)$$

This value agrees, within experimental error, with $g = 2.93$ obtained for the Γ_6 triplet exciton absorption band^{7,8} and confirms the assignment of the luminescence lines mentioned above.

2. $\vec{H} \parallel \vec{c}$, $\vec{E} \perp \vec{c}$, and $\vec{k} \parallel \vec{c}$ reflectance

For an evaluation of the electron and hole g values $g_{e\parallel}$ and $g_{h\parallel}$, the difference $g_{h\parallel} - g_{e\parallel}$ has to be determined in addition to $|g_{h\parallel} + g_{e\parallel}|$. According to Table III, $g_{h\parallel} - g_{e\parallel}$ can be deduced from the splitting of the $\Gamma_5 A$ -exciton states for $\vec{H} \parallel \vec{c}$. High-quality vapor-grown crystal platelets always have the c axis in the plane of the platelet. As a consequence, observation of photons emitted with wave vector perpendicular to the surface of the

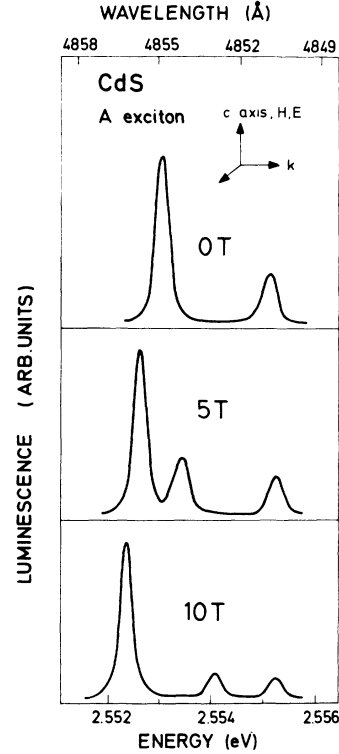


FIG. 1. Magnetoluminescence of Γ_6 triplet and Γ_{5L} longitudinal A-exciton states of CdS at 4°K for $\vec{H} \parallel \vec{c}$ and $\vec{E} \parallel \vec{c}$.

platelets always corresponds to Voigt configuration, if H is along the c axis. In Voigt configuration no splitting of the $\Gamma_5 A$ -exciton state could be observed. This is interpreted as a quenching of the linear Zeeman splitting due to the large longitudinal-transverse (LT) splitting [see Sec. III, Eqs. (3.7) and (3.11)]. In fact, the LT splitting is ~ 2 meV, determined by comparison between calculated and experimentally observed reflectance line shape, already shown for example in Ref. 15. Associating the energy separation between the Γ_{5L} ($\vec{E} \parallel \vec{c}$) and Γ_{5T} ($\vec{E} \perp \vec{c}$) luminescence maxima with the LT splitting gives a similar value. However, one has to keep in mind that the luminescence maximum observed for $E \perp c$ polarization does not really give the Γ_{5T} energy due to the polariton effect, which in the present case even shifts the Γ_{5T} -luminescence maximum slightly below the Γ_6 luminescence maximum.

Experiments in Faraday configuration require observation of the luminescence from the edge of the platelets or, alternatively, measurements on as grown surfaces perpendicular to the c axis of larger crystals. We chose the second alternative and determined $g_{h\parallel} - g_{e\parallel}$ from magnetoreflectance

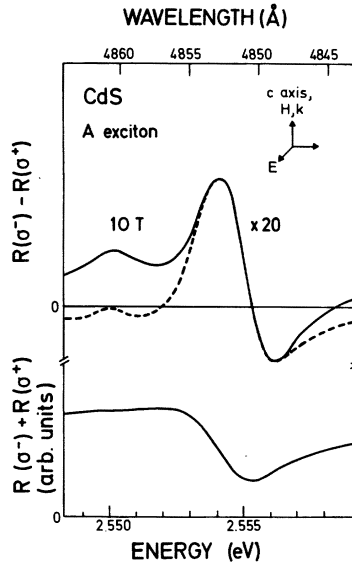


FIG. 2. Sum (lower curve) and difference (solid curve, upper part) of σ^- and σ^+ reflected light at 4°K. σ^- corresponds to an excited state with $m_j = -1$. Dashed curve: calculated difference spectrum corresponding to $g_{h\parallel} - g_{e\parallel} = -0.56$.

measurements.

We simultaneously measured the difference $R_{\text{diff}}(E) = R_{\sigma^-}(E) - R_{\sigma^+}(E)$ and the sum $R_{\text{sum}}(E) = R_{\sigma^-}(E) + R_{\sigma^+}(E)$ of left-circular-polarized (LCP) and right-circular-polarized (RCP) reflected light, R_{σ^-} and R_{σ^+} , respectively. Assuming the same line shape for R_{σ^-} and R_{σ^+} and a relative shift $\Delta E = g\mu_B H$ between R_{σ^-} and R_{σ^+} , the g value to be evaluated is determined by the requirement

$$R_{\text{diff}}(E) = R_{\sigma^-}(E) - R_{\sigma^-}(E - \Delta E) \\ = -\frac{dR_{\sigma^-}}{dE} \Delta E = -\frac{dR_{\sigma^-}}{dE} g\mu_B H. \quad (4.3)$$

As long as ΔE is small compared to the half-width of the reflectance structure, R_{σ^-} may be replaced by $\frac{1}{2}R_{\text{sum}}$, otherwise R_{σ^-} has to be measured separately and its intensity calibrated properly. The best agreement between the R_{diff} spectrum and the curve calculated from Eq. (4.3) is obtained for

$$g_{h\parallel} - g_{e\parallel} = -0.56 \pm 0.05 \quad (4.4)$$

as shown in Fig. 2.

Two remarks should be made on the results shown in Fig. 2. (a) The difference between R_{diff} as measured experimentally and the calculated curves at high energies is attributed to the B exciton. The B exciton, which is ~ 16 meV above the A exciton, has a positive g factor, raising the relative intensity of the LCP reflected light intensity with respect to the RCP light intensity on the low-energy side of the B exciton, i.e., on the high-en-

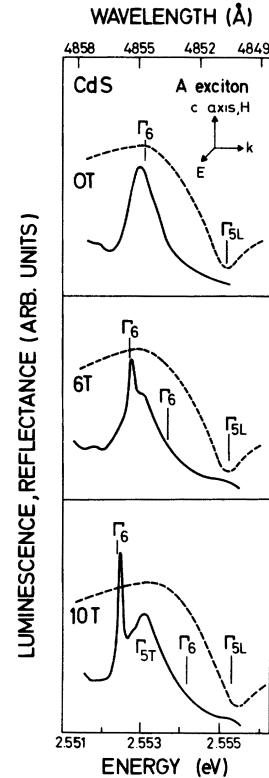


FIG. 3. Magnetoluminescence (solid line) and magnetoreflectance (broken line) of CdS for $\vec{H} \parallel \vec{c}$, $\vec{E} \perp \vec{c}$, and $\vec{k} \perp \vec{c}$ at 4°K.

ergy side of the A exciton, and this has been neglected in the calculation of the theoretical curves in Fig. 2. (b) The deviations of the calculated curves from the experimental one at low energies may be due to the influence of bound excitons. The additional structure at 2.550 eV is also attributed to a bound exciton state, since many crystals exhibit a corresponding luminescence structure of comparable half-width in this energy region. The derivative spectrum in Fig. 2 looks similar to recently published magnetoreflectance data on CdS with field modulation, where an additional structure below the Γ_5 exciton state was attributed to the Γ_6 triplet state.¹⁶ The energy separation between the Γ_5 and Γ_6 states in Ref. 16 are in accordance with the present experiments. On the other hand, the 2.550-eV structure as given in Fig. 2 cannot be explained along similar lines, since both the line shape and the energy position could not be explained attributing the structure to the Γ_6 triplet state.

From (4.2) and (4.4) $g_{h\parallel}$ and $g_{e\parallel}$ can be derived immediately. Assuming $|g_{e\parallel}| > |g_{h\parallel}|$ one gets

$$g_{e\parallel} = +1.79 \pm 0.10, \quad (4.5)$$

$$g_{h\parallel} = +1.23 \pm 0.10. \quad (4.6)$$

These values are in close agreement with $g_{e\parallel} = -1.78$ and $g_{n\parallel} = -1.15$ as given in Ref. 8, where the difference in sign is due to a different definition of the g factor (free-electron g factor of -2 in Ref. 8 in contrast to $+2$ in the present paper).

3. $\vec{H}\parallel\vec{c}$, $\vec{E}\perp\vec{c}$, and $\vec{k}\perp\vec{c}$ luminescence

Luminescence spectra for $\vec{H}\parallel\vec{c}$, $\vec{E}\perp\vec{c}$, and $\vec{k}\perp\vec{c}$ exhibit strong magnetic-field-dependent changes in the region of the A exciton in contrast to the small changes in the corresponding reflectance spectra as shown in Fig. 3. A narrow line emerges on the low-energy side of the luminescence maximum due to the Γ_5 state. With increasing magnetic field its intensity relative to that of the Γ_{5T} luminescence line increases and the energy separation between both lines becomes larger. The energy position of the additional line cannot be traced below 5 T but extrapolation of the high-field data leads to an energy position close to the Γ_5 luminescence peak at zero magnetic field.

Comparison between the $\vec{E}\perp\vec{c}$ and $\vec{E}\parallel\vec{c}$ polarized luminescence for $\vec{H}\parallel\vec{c}$ reveals that the additional line in the $\vec{E}\perp\vec{c}$ polarized spectrum occurs at the energy of the low-energy triplet component observed for $\vec{E}\parallel\vec{c}$, and thus the narrow $\vec{E}\perp\vec{c}$ polarized line is attributed to the lower-energy Γ_6 triplet component.

An alternative interpretation of the two lines observable at high magnetic fields as the two Zeeman components of the $\Gamma_5 A$ -exciton state is rejected for the following reasons: In the case of linear Zeeman splitting of the Γ_5 state observed in Voigt configuration one of the Zeeman components should converge to the longitudinal exciton energy at zero magnetic field and the energy separation of the two components should always be larger than the LT -splitting. Also, one would expect a similar line shape at higher magnetic fields for the two Zeeman components, whereas the low-energy line is much narrower than the higher-energy line in the present case. Finally, the energy separation between the lines is much larger than that calculated with the g factor derived from the reflectance measurements. Hence, we conclude that the additional line does not correspond to the $\Gamma_5 A$ -exciton state, but to the Γ_6 state as already stated.

The selection rule for the Γ_6 state was discussed in Sec. III C 2. Among various possibilities of perturbation-induced transfer of oscillator strength to the Γ_6 state the most likely one is the mixing mechanism due to nonzero wave vector k_x, k_y in a configuration $\vec{k}\perp\vec{c}$, $\vec{E}\perp\vec{c}$, $\vec{H}\parallel\vec{c}$ and without external electric field or stress. The contribution from the k -linear mixing mechanism is obtained replacing H_x, H_y in Table III by $-k_y, k_x$ and at the same time

regarding the quantities $\mu_B g_i$ as effective parameters for this new matrix. The terms including g_{\perp} come from the conduction band and can be regarded as very small. Terms with the coefficient g_4 , however, could make appreciable contributions, because the same coefficient appears for the mixing of $\Gamma_{5L}(A)$ and $\Gamma_1(B)$ and it is generally accepted that the appearance of the $\Gamma_{5L}(A)$ state for $\vec{E}\parallel\vec{c}$ and $\vec{k}\perp\vec{c}$ is due to this mixing.⁸ Besides the mixing mechanism due to nonzero wave vector k_x, k_y , other possible, but less-likely perturbations which could make the triplet state observable are finite electric field E or strain field ϵ associated with phonons or internal strain.

Wave vector-induced mixing between A - and B -exciton states is independent of the applied magnetic field, and the magnetic field dependence of the Γ_6 line intensity can be explained in the following way: For $H=0$ the Γ_5 and Γ_6 states are nearly degenerate, and due to its low oscillator strength the Γ_6 line is hidden in the intense Γ_5 luminescence. With increasing magnetic field, $\vec{H}\parallel\vec{c}$, the Γ_5 and Γ_6 states both split into two components, and due to the considerably larger g value of the Γ_6 state compared to that of the Γ_5 state, one Γ_6 component is shifted to energies below the Γ_5 states. Thermalization then favors a larger population of the low-energy Γ_6 component and moreover the probability for a polariton in the crystal to be converted into a light quantum outside the crystal is larger for the Γ_6 low-energy component than for the Γ_5 state. The same arguments used to explain the appearance of the low-energy Γ_6 component for $E\perp c$ polarization also explain the nonobservability of the high-energy Γ_6 component: This state is shifted above the two Γ_5 components, and in this case thermalization tends to decrease the relative intensity of this line and the conversion rate from a polariton to a light quantum outside the crystal is low.

4. $\vec{H}\parallel\vec{c}$, $\vec{E}\perp\vec{c}$, and $\vec{k}\parallel\vec{c}$ luminescence

Luminescence spectra for $\vec{H}\parallel\vec{c}$ and $\vec{E}\perp\vec{c}$ were also measured in Faraday configuration, i.e., in the same configuration as the reflectance presented in Sec. IV A 2. The luminescence results are similar to those shown in Fig. 3. However, they cannot simply be explained in exactly the same way, but some additional scattering processes between the Γ_5 and Γ_6 exciton states are required. The origin of this scattering could be manifold: impurities, phonons, internal stress, etc. The appearance of the state might even be explained by one of the scattering processes alone without k -linear mixing, but this seems to be unlikely. For example, if we assume the existence of ϵ_{xx} -type in-

ternal strain in all measurements, this would explain the results, but it seems to be a rather odd assumption that such strain should be present in all samples, grown by different methods and by different crystal growers. Within experimental error no temperature dependence of the mixing could be observed for $4 < T < 30$ °K, and this is against an interpretation of the results as essentially due to phonons, and thus scattering by impurities in addition to the k -linear mixing mechanism remains the most plausible explanation. The observed broadening of the Γ_6 luminescence line with increasing distance of the excitation spot from the edge of the platelet, where the luminescence is observed, indicates the importance of scattering, although we cannot determine uniquely at present the scattering process responsible for the appearance of the Γ_6 state in both configurations $\vec{k} \parallel \vec{c}$ and $\vec{k} \perp \vec{c}$ (for $\vec{E} \perp \vec{c}$ and $\vec{H} \parallel \vec{c}$).

5. $\vec{E} \parallel \vec{H} \perp \vec{c}, \vec{k} \perp \vec{c}$

In addition to the experiments with applied magnetic field $\vec{H} \parallel \vec{c}$ we also investigated the luminescence and reflectance of the A exciton in a magnetic field $\vec{H} \perp \vec{c}$. (Corresponding reflectance spectra were already shown in Ref. 10).

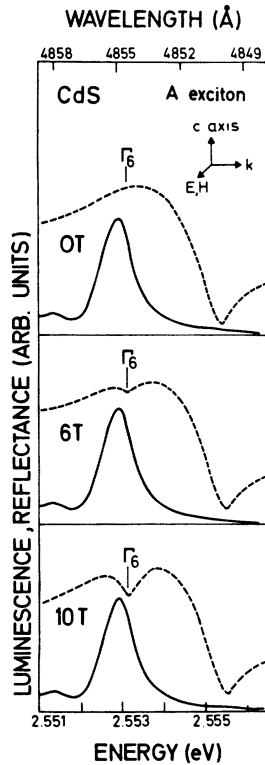


FIG. 4. Magnetoluminescence (solid line) and magnetorefectance (broken line) of CdS for $\vec{H} \perp \vec{c}$, $\vec{E} \perp \vec{c}$, and $\vec{k} \perp \vec{c}$ at 4 °K.

The most prominent feature of the reflectance spectrum is the occurrence of an additional reflectance minimum with increasing magnetic field. The additional structure appears below the main reflectance minimum at the energy of the Γ_5 transverse state, where the Γ_6 luminescence line is observed for $\vec{E} \parallel \vec{c}$ polarization. Thus, the additional reflectance structure is attributed to the Γ_6 triplet state which becomes observable through a mixing of the Γ_5 and Γ_6 exciton states induced by the magnetic field $\vec{H} \perp \vec{c}$. This mixing by H -dependent off-diagonal terms in the A -exciton submatrix can be seen in Table III.

Luminescence measured in the same configuration did not show, even at highest magnetic fields, any additional structure corresponding to the radiative decay of the Γ_6 A -exciton state. This might appear surprising when compared to the case of much weaker coupling discussed before ($\vec{H} \parallel \vec{c}$, $\vec{E} \perp \vec{c}$), where no Γ_6 related structure could be observed in reflectance, while the luminescence spectrum exhibited a pronounced Γ_6 line. However, the important difference between the two cases is the fact that for $\vec{H} \perp \vec{c}$ no splitting of the Γ_5 and Γ_6 states occurs, and as a consequence no shift of a Γ_6 component below the energy of the Γ_5 states. Thus the luminescence of the Γ_6 state, which is partly allowed due to the mechanism outlined in Sec. III C always overlaps with the luminescence of the Γ_5 state and is not observed separately.

6. Diamagnetic shift of Γ_6 state

In addition to the splitting and mixing of the exciton states the magnetic field introduces a diamagnetic shift, which can be measured best for the Γ_6 state due to the sharpness of the corresponding luminescence line(s). For $\vec{H} \parallel \vec{c}$ the center of the two split Γ_6 components exhibits a diamagnetic shift of 0.22 ± 0.03 meV at 100 kG. From this we calculate a reduced exciton mass

$$\mu_x = 0.16 \pm 0.03 \quad (4.7)$$

according to Table II and Eq. (3.2), using $\epsilon_{\text{oll}} = 8.64$ and $\epsilon_{\text{ol}} = 8.28$.¹⁷ The value for μ_x is the same as given in Ref. 8, however, in that case μ_x was derived with $\epsilon_{\text{oll}} = 9.58$ and $\epsilon_{\text{ol}} = 9.02$. Taking these values for the dielectric constant we would get $\mu_x = 0.17$. However, we prefer the value given above, since a lower value for the dielectric constant seems to be more appropriate (cf., for example, Refs. 18 and 19).

For $\vec{H} \perp \vec{c}$, the Γ_6 line does not split, but exhibits a diamagnetic shift of 0.19 ± 0.03 meV at 100 kG. Comparison with the diamagnetic shift measured for $\vec{H} \parallel \vec{c}$ yields according to Eq. (3.3) and Table II

$$\mu_x = 0.185 \pm 0.03 \quad (4.8)$$

This again is in close agreement with the value $\mu_x = 0.19$ as given in Ref. 8. Thus our experiments support the electron effective masses $m_{e\parallel}^* = 1.98m_0$ and $m_{e\perp}^* = 0.209m_0$,⁸ in combination with the hole effective masses $m_{h\parallel}^* = 5.0m_0$ and $m_{h\perp}^* = 0.7m_0$,²⁰ but our results do not support the $\sim 20\%$ smaller electron effective masses as given in Ref. 21.

B. CdSe

In addition to the experiments on CdS, magnetoluminescence and magnetorefectance were also measured on CdSe in the region of the A exciton.

For $\vec{E}\parallel\vec{c}$ polarization one single luminescence peak is observed at 1.8261 eV for zero magnetic field. This peak does not split under the influence of a magnetic field parallel to the c axis even at 100 kG (similar to the high-energy component in the $\vec{E}\parallel\vec{c}$ polarized spectra of CdS, cf. Fig. 1). The peak intensity increases strongly if the photon wave vector k deviates from the direction perpendicular to the c axis. Thus this maximum is attributed to the longitudinal state of the A exciton.

Luminescence spectra with $\vec{E}\perp\vec{c}$ polarization (see Fig. 5, solid curves) are characterized at zero magnetic field by two sharp maxima around 1.824 eV, corresponding to bound excitons, and a broader maximum between 1.825 and 1.827 eV, attributed to luminescence from the Γ_5 state of the A exciton.

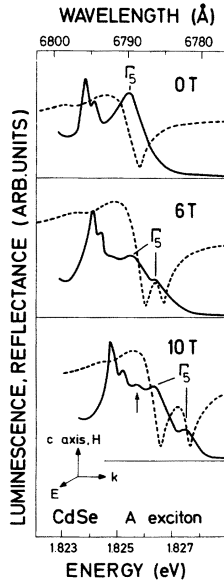


FIG. 5. Magnetoluminescence (solid line) and magnetorefectance (dashed line) of CdSe for $\vec{H}\parallel\vec{c}$, $\vec{E}\perp\vec{c}$, and $\vec{k}\perp\vec{c}$ at 4°K. The luminescence structure at 6795 Å corresponds to bound excitons. The arrow indicates a state tentatively attributed to the Γ_6 triplet state.

In the presence of a magnetic field parallel to the c axis the Γ_5 transverse state splits into two components. CdSe, like CdS, tends to form thin crystal platelets having the c axis within the plane of the crystal, and thus for $\vec{H}\parallel\vec{c}$ observation with k perpendicular to the crystal surface corresponds to Voigt configuration. Crystals having sufficiently large surfaces perpendicular to the c axis suitable for observation in Faraday configuration with $\vec{H}\parallel\vec{c}$ were not available and in consequence we determined the g value of the Γ_5 state from luminescence measurements in Voigt configuration.

We derived

$$|g_{h\parallel} - g_{e\parallel}| = 1.76 \pm 0.20 \quad (4.9)$$

from the change of the energy separation between the two Γ_5 components at high magnetic fields (see Fig. 5). At lower fields the splitting is not a linear function of H , since the Zeeman splitting and the LT splitting are of comparable magnitude (a line-shape fit of the zero-field reflectance curve yields an LT splitting of ~ 1 meV).

In addition to the Γ_5 Zeeman doublet and the two bound exciton lines a third rather flat peak is observed between the free and bound exciton lines at high magnetic fields. The energy of this peak converges to an energy below that of the Γ_5 luminescence maximum at $H = 0$, but higher than the energy of the bound exciton lines. Thus one may attribute this additional structure to the Γ_6 triplet state. Any definite conclusion, however, concerning this particular point, requires more experimental support than the present data.

The diamagnetic shift of the Γ_5 A-exciton state was 1.45 meV for $\vec{H}\parallel\vec{c}$ at 100 kG giving a reduced exciton mass

$$\mu_x = 0.096 \pm 0.010, \quad (4.10)$$

using $\epsilon_{0\parallel} = 9.25$ and $\epsilon_{0\perp} = 8.75$.¹⁷ For $\vec{H}\perp\vec{c}$ the diamagnetic shift was 1.24 meV at 100 kG, giving for the ratio of the effective masses in the x and z direction [according to (3.3) and Table II]:

$$\mu_x/\mu_z = 0.86 \quad (4.11)$$

which finally yields

$$\mu_z = 0.112 \pm 0.010. \quad (4.12)$$

All values are in good agreement with those derived from magnetoabsorption by Wheeler and Dimmock,⁹ who obtained $\mu_x = 0.100$ and $\mu_z = 0.130$.

The magnetorefectance spectra for $\vec{H}\parallel\vec{c}$ are given by the broken lines in Fig. 5. Due to the smaller LT splitting and the larger g value of the Γ_5 state of CdSe compared to CdS, where no splitting of the Γ_5 state could be observed even at 12 T, two reflectance minima are already observed at 4 T in the case of CdSe.

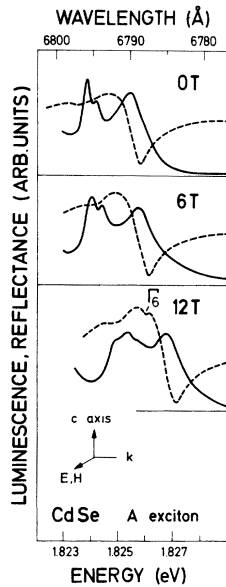


FIG. 6. Magnetoluminescence (solid line) and magnetoreflectance (dashed line) of CdSe for $\vec{H} \perp \vec{c}$, $\vec{E} \perp \vec{c}$, and $\vec{k} \perp \vec{c}$.

For $\vec{H} \perp \vec{c}$ no splitting of the Γ_5 state, but a mixing of the Γ_5 and Γ_6 states of the A exciton is expected (cf. Table III). In luminescence with $\vec{E} \perp \vec{c}$ polarization no change of the spectra could be observed in the region of the A exciton, but in reflectance a weak additional structure below the main reflectance minimum becomes observable at highest magnetic fields (see Fig. 6), and this structure is attributed to the Γ_6 triplet state. The weakness of the Γ_6 state indicates that the mixing between the Γ_5 and Γ_6 A-exciton states is weaker in CdSe than in CdS.

V. SUMMARY

We investigated the behavior of the A exciton in CdS and CdSe under the influence of a magnetic field up to 12 T. In the case of CdS, we derived $|g_{h\parallel} + g_{e\parallel}| = 3.02 \pm 0.1$ from the splitting of the Γ_6

state for $\vec{H} \parallel \vec{c}$, while the directly measured difference between σ^+ and σ^- polarized reflected light yields the g factor of the Γ_5 state $g_{h\parallel} - g_{e\parallel} = -0.56 \pm 0.05$. From these values the electron and hole g values are determined as $g_{e\parallel} = +1.79 \pm 0.1$ and $g_{h\parallel} = +1.23 \pm 0.1$. The diamagnetic shift of the Γ_6 state yields reduced exciton masses $\mu_x = 0.16 \pm 0.02$ and $\mu_z = 0.18_5 \pm 0.02$.

For CdSe the splitting of the Γ_5 luminescence peak for $\vec{H} \parallel \vec{c}$ yields $|g_{h\parallel} - g_{e\parallel}| = +1.76 \pm 0.1$. The magnetoreflectance spectra exhibit a splitting into two components, and their energy separation is in accordance with the g value derived from the luminescence data. From the diamagnetic shift of the A exciton we derive the reduced exciton masses $\mu_x = 0.096 \pm 0.01$ and $\mu_z = 0.112 \pm 0.01$.

All values are in quantitative agreement with data reported in the literature, which were derived from magneto-optical investigations of excited states ($n \geq 2$).

The Γ_6 triplet state of the A exciton was observed with $\vec{E} \perp \vec{c}$ polarization. A magnetic field $\vec{H} \perp \vec{c}$ mixes the Γ_5 and Γ_6 A-exciton states and the dipole-forbidden Γ_6 state gets sufficient oscillator strength to produce an extra reflectance structure. The effect is more pronounced in CdS than in CdSe.

In CdS the Γ_6 state is also observed in luminescence for $\vec{E} \perp \vec{c}$ and $\vec{H} \parallel \vec{c}$. In this configuration the Γ_6 state of the A exciton gets oscillator strength from the B exciton and becomes observable as a separate luminescence line, since the magnetic field $\vec{H} \parallel \vec{c}$ shifts one Γ_6 component below both Γ_5 Zeeman components. The mixing is too weak to produce a corresponding reflectance structure for this configuration.

ACKNOWLEDGMENTS

The authors thank Mrs. R. Broser for kindly providing large high-quality CdS crystals and high-quality CdSe platelets, and we thank R. Humphreys for a critical reading of the manuscript, and acknowledge the expert technical assistance by H. Hirt, G. Wolf, and P. Wurster.

*Present address: The Institute for Solid State Physics, The University of Tokyo, Roppongi, Minato-ku, Tokyo, Japan.

†Present address: Faculty of Engineering Science, Osaka University, Toyonaka, Osaka, Japan.

¹S. Permogorov, Phys. Status Solidi B **68**, 9 (1975).

²P. Wiesner and U. Heim, Phys. Rev. B **11**, 3071 (1975).

³H. Sumi, Solid State Commun. **17**, 701 (1975).

⁴S. Suga, K. Cho, and P. Hiesinger, J. Lumin. **12/13**, 109 (1976).

⁵S. Shionoya, H. Saito, E. Hanamura, and O. Akimoto,

Solid State Commun. **12**, 223 (1973).

⁶J. Voigt, F. Mir and G. Kehrberg, Phys. Status Solidi B **70**, 625 (1975).

⁷R. G. Wheeler and J. O. Dimmock, Phys. Rev. Lett. **3**, 372 (1959).

⁸J. J. Hopfield and D. G. Thomas, Phys. Rev. **122**, 35 (1961).

⁹R. G. Wheeler and J. O. Dimmock, Phys. Rev. **125**, 1805 (1962).

¹⁰S. Suga, M. Bettini, W. Dreybrodt, and K. Cho, Colloq. Int. Cent. Natl. Rech. Sci. No. **242**, 217 (1975).

- ¹¹K. Cho, Phys. Rev. B 14, 4463 (1976).
- ¹²L. C. Greene and C. R. Geesner, J. Appl. Phys. 38, 3662 (1967).
- ¹³L. C. Greene and H. A. Wilson, J. Appl. Phys. 42, 2758 (1971).
- ¹⁴D. G. Thomas and J. J. Hopfield, Phys. Rev. 128, 2135 (1962).
- ¹⁵J. J. Hopfield and D. G. Thomas, Phys. Rev. 132, 563 (1963).
- ¹⁶G. Gatti, M. Iannuzzi, and V. Montelatici, Solid State Commun. 19, 823 (1976).
- ¹⁷B. Segall and D. T. F. Marple, *Physics and Chemistry of II-VI compounds*, edited by M. Aven and J. S. Prener (North-Holland, Amsterdam, 1967) p. 319.
- ¹⁸S. A. Permogorov, V. V. Travnikov, and A. V. Sel'kin, Fiz. Tverd. Tela 14, 3642 (1972) [Sov. Phys.-Solid State 14, 3051 (1973)].
- ¹⁹J. Voigt, M. Senoner and I. Rückmann, Phys. Status Solidi B 75, 213 (1976).
- ²⁰G. D. Mahan and J. J. Hopfield, Phys. Rev. 135, A428 (1964).
- ²¹R. Levi, A. Bivas, J. B. Grun, and S. Nikitine, Springer Tracts Mod. Phys. 73, 171 (1975).